OBSERVATIONS OF VEHICLE SURFACE CHARGING IN DUSTY PLASMA

Aroh Barjatya
ECE Dept, Utah State University, 4120 Old Main Hill, UT 84322
Phone: (435) 881-1616
E-mail: arohb@cc.usu.edu

Dr. Charles M. Swenson
ECE Dept, Utah State University

Abstract

The NASA Sudden Atom Layer (SAL) rocket was launched in February of 1998 from Puerto Rico into an approximately 5 km thick sodium layer that peaked at 94 km altitude. This layer was observed from ground based sodium lidar as well as the Arecibo Radar. The instrument payload consisted of a charged dust detector, an electric field probe, a DC Langmuir probe, and a RF impedance probe. The instruments experienced an anomalous charging event as the rocket passed through this sodium layer. We present here an analysis of the DC Langmuir probe data and the RF impedance probe data to compute the amount of vehicle charging attributed to charged dust. Possible scenarios that could lead to the observed charging effects on the instruments are investigated using a novel SPICE model. The model development and its features are also presented in this paper.

Introduction

Since the first report on charging of the spacecraft surface in geosynchronous orbit [DeForest, 1972] and the subsequent realization that charging could lead to serious operational anomalies [Rosen, 1976], the understanding of spacecraft charging has increased significantly [Garrett and Whittlesey, 2000]. Although the low Earth orbits (LEO) are largely immune to charging due to higher ambient plasma density, analysis of a series of DMSP satellites has proved that high latitude LEO is subject to severe kilovolt charging, lasting tens of seconds [Gussenhoven et al, 1985; Frooninckx and Sojka, 1992].

All the above scenarios pertain to satellites and interplanetary spacecrafts flying through hot collision-less plasma with little or no dust present in the environment. The 80-100 Km altitude range, where most of the sounding rockets fly, presents a different charging dynamics situation then the one present at 'satellite orbit' altitudes. The difference is manifested by enormous amount of meteoric material that condenses into dust particles and is suspended in the Earth's mesosphere between 80-100 Km. The presence of dust at such a low altitude where the Debye length and the mean free path is small, constitutes a "dusty plasma", as compared to the "dust in plasma" at higher 'satellite orbit' altitudes. The Earth's atmosphere at these low altitudes also presents us with anomalous physical phenomena like noctilucent clouds, polar summer mesospheric echoes (PMSE) and sporadic sodium layers. The occurrence of each of these phenomena has been researched extensively in the literature, and in some or the other way each of these phenomena has been linked with the presence of charged dust in the lower Earth atmosphere.

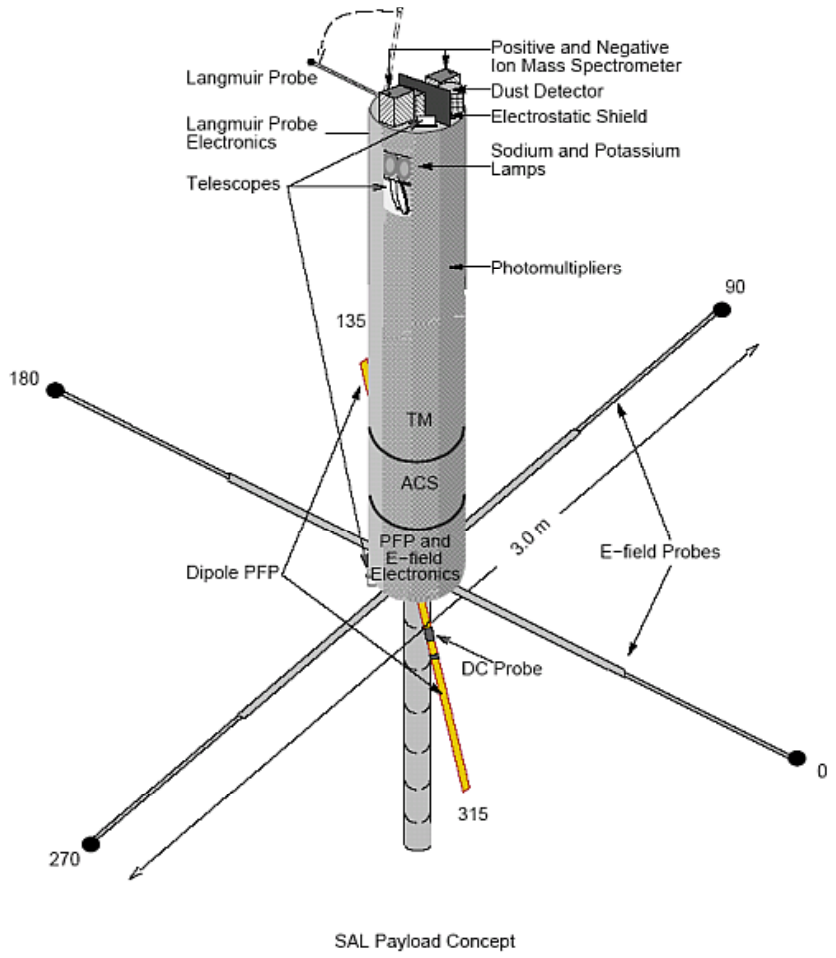

Figure 1. The Sudden Atom Layer Rocket (NASA 21.117) was launched February 20, 1998 at 2009 Local Time. This Cornell University payload included instruments from Utah State University, University of New Hampshire, Naval Research Labs, NASA and Aerospace Corporation.

One of the ways to settle these speculations is to perform in-situ observations of the atmosphere when these anomalies occur. The NASA Sudden Atomic Layer investigation sounding rocket program [Gelinas et al, 1998] was such an attempt to facilitate an understanding of the sporadic sodium layers. The rocket flight detected a layer of charged dust near a sporadic sodium layer. Amongst the large instrument suite that the rocket carried, it carried a radio frequency Swept Impedance Probe (SIP) for absolute electron density measurement and a DC Langmuir Probe (DCP) for relative electron density measurements. There was a significant disagreement between the two probes during a short phase of the flight. The data points to a case of rocket surface charging which the DCP is sensitive to and the SIP insensitive to.

A significant amount of mathematical modeling work has been done in literature to understand the behavior of a spacecraft during charging incidences. Although for a detailed spacecraft-specific analysis tedious mathematical modeling is imperative, for just understanding the behavior of spacecraft at a higher level, a simpler approach is desired.

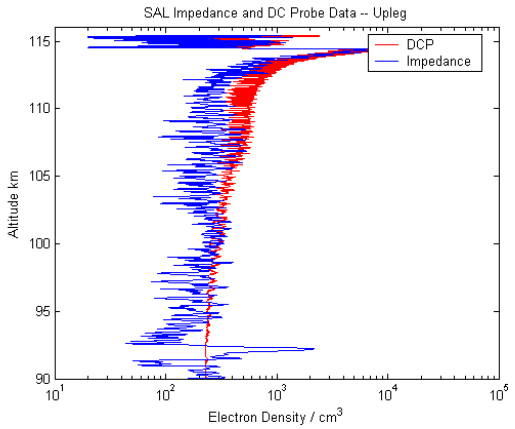

Figure 2(a). Upleg trajectory electron density profile

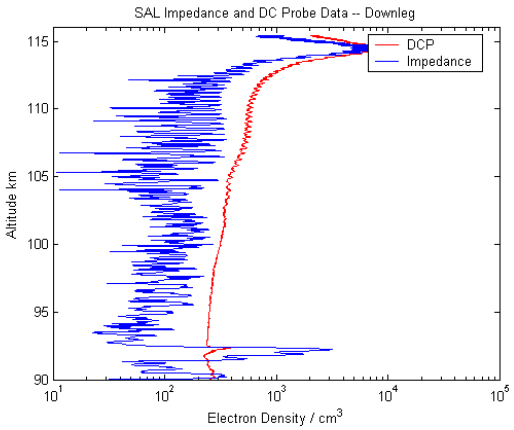

Figure 2(b). Downleg trajectory electron density profile.

In this work we first give an overview of the NASA Sudden Atom Layer (SAL) rocket payload along with the data from the SIP and the DCP. We then develop a simple SPICE (Simulation Program with Integrated Circuit Emphasis) model that can be used to simultaneously calculate spacecraft floating potential and instrument response using the numerical solvers available within SPICE. SPICE is an industry standard simulation program used by electrical engineers for simulating networks of linear and non-linear circuit elements [Keown, 2001]. This model is then applied to the SAL scenario in order to understand the anomaly observed in the DCP data.

Sudden Atom Layer (SAL) Investigation.

Cornell Universities Sudden Atomic Layer (SAL) Investigation sounding rocket was launched from Puerto Rico on 19 Feb 1998 at 2009 LT. The rockets main scientific goal was the investigation of the phenomenon of sporadic sodium layers (Na_s), which are thin (1 Km) layers of neutral atomic metal that form in the mesosphere, roughly at an altitude of 90-100 Km. The payload is as shown in Figure 1. The payload instruments included a charged dust detector to measure mesospheric dust over a mass range of 1,000 –10,000 amu, a Langmuir probe operating as Fast Temperature Probe to measure plasma temperature, electric field booms to measure fields from DC to 5 KHz, telescopes to measure sodium airglow, photometers and lamps to measure neutral sodium and potassium densities, a positive ion mass spectrometer, and a Swept Impedance Probe (SIP) & DC Langmuir Probe (DCP) to measure the absolute and relative electron density respectively.

The SAL rocket flight reached a maximum altitude of 115.5 Km and flew through two thin Na_s layers at 94 Km and 97 Km, with peak densities of 6000 cm^{-3} and 4000 cm^{-3}, as determined by the Arecibo sodium resonance density lidar. The dust detector observed a positive dust layer at the bottom of the lower Na_s layer at 92 Km altitude [Gelinas et al, 1998]. The SIP, provided by Utah State University/Space Dynamics Lab, successfully measured electron density and the measurement techniques included in this version of the probe provided valuable insight into electron density structures associated with sudden sodium layers. The SIP recorded a high electron density layer at 92 Km and an intermediate layer at 114 Km. The SIP data is shown in

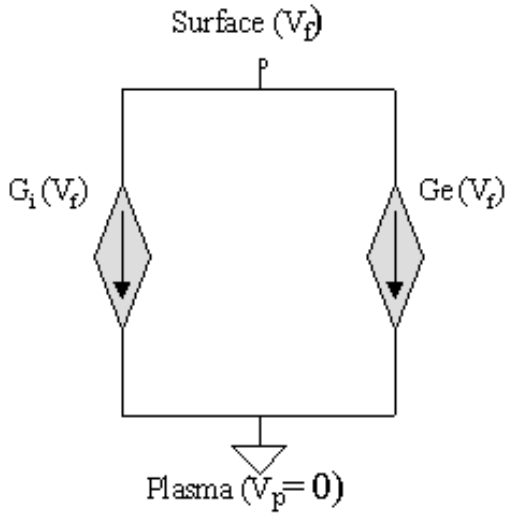

Figure 3. The SPICE sub-circuit Model for a generic spacecraft

Figure 2. Also shown is the DC Langmuir probe relative density data that has been normalized to the SIP data at 114 Km altitude. The important point to note is that the DC Langmuir probe completely missed the 92 Km electron density layer in the rockets upleg trajectory and registered a faint signal on the downleg trajectory. Although at first sight itself we realize that this is related to rocket surface charging, but the relation of charging to the presence of charged dust is unknown and we also do not realize the reason as to why a faint signal was observed in the downleg trajectory and almost nothing on the upleg. We now present a simple charging model to analyze this problem at a very crude level.

Model Development

A Maxwell-Boltzmann distribution is assumed for electrons and ions. The basic process behind spacecraft charging is that of current balance at equilibrium, i.e. all currents must sum to zero. The potential at which this is achieved is the potential difference between the spacecraft surface and the space plasma ground. The former is referred to as the floating potential of the spacecraft surface and the latter as plasma potential. The equation expressing this current balance can be stated as:

$$I_E(V) - [I_I(V) + I_{SE}(V) + I_{BSE}(V) + I_{PH}(V) + I_B(V)] = I_T \qquad (1)$$

Where

V	Spacecraft potential	I_{BSE}	Back-scatter electron current
I_E	Electron current to spacecraft surface	I_{PH}	Photo-electron current
I_I	Ion current to spacecraft surface	I_B	Active current sources such a ion beams
I_{SE}	Secondary electron current	I_T	Total current (= 0 at equilibrium)

In this paper the plasma potential will be taken as zero and hence as circuit electrical ground in the SPICE model. A SPICE sub-circuit model, as shown in Figure 2, can be conceptualized

considering only the positive electron current (current going out) and the negative ion current (current coming in) and disregarding all other currents given in equation (1). Each of these current sources is modeled as a voltage-controlled-current-source (VCCS), since both the ion and electron currents are dependent on the potential of the spacecraft with respect to the plasma. In this paper VCCS is represented as G (V), keeping in line with the syntax used in SPICE. Hence, ion current is written as $G_i(V_f)$ and electron current as $G_e(V_f)$, where V_f is the potential of the spacecraft surface.

The sub-circuit is modeled using SPICE 'Analog Behavioral Modeling' features, that allow an entire equation governing the behavior of the circuit to be modeled. Our model, as a first step, models $G_i(V_f)$ and $G_e(V_f)$ with the retardation and saturation region equations for a cylindrical Langmuir probe in collision-less plasma.

For relative potential of the surface with the plasma greater than zero, the electron current is referred to be as being in the saturation region. The ions, however, are retarded by the positive potentials, leading to an exponential decrease in the ion current as the potential increases. The opposite is true when the potential is negative, the ion current referred to as being in saturation region while the electron current in retardation region.

The current equation for electrons [Chen, 1965; Pfaff, 1996] is given as follows, where the first equation governs the current in saturation region and the second one in retardation region. The ion current is governed by similar equations except that the relational condition for spacecraft potential V with respect top plasma potential V_p and the direction of current, both are reversed.

$$G_e(V) = An_o e\sqrt{\frac{k_b T_e}{2\pi m_e}}\sqrt{\left(1+\frac{e(V-Vp)}{k_b T_e}\right)} \quad V \geq V \tag{2}$$

$$G_e(V) = An_o e\sqrt{\frac{k_b T_e}{2\pi m_e}}\exp\left(\frac{e(V-Vp)}{k_b T_e}\right) \quad V \leq Vp \tag{3}$$

Where

A	Surface area	T_e	Electron temperature
n_o	Plasma density	V	Surface potential
e	Fundamental charge	V_p	Plasma potential (taken by model as 0)
k_b	Boltzmann Constant	m_e	Electron mass

These equations are then solved to find out the floating potential of the spacecraft. In earlier similar models developed, that constitute multiple numbers of such current sources [Smithtro and Swenson, 2002] the equations are solved for V_x, where x stands for a particular instance of the current source, and then the resulting expression simulated using commercially available mathematical tools to find the floating potential of all the elements in the model. The benefit of using SPICE for modeling these equations is that the SPICE software itself solves for V, while doing a bias-point analysis, giving the floating potential of the surface, such that the total current

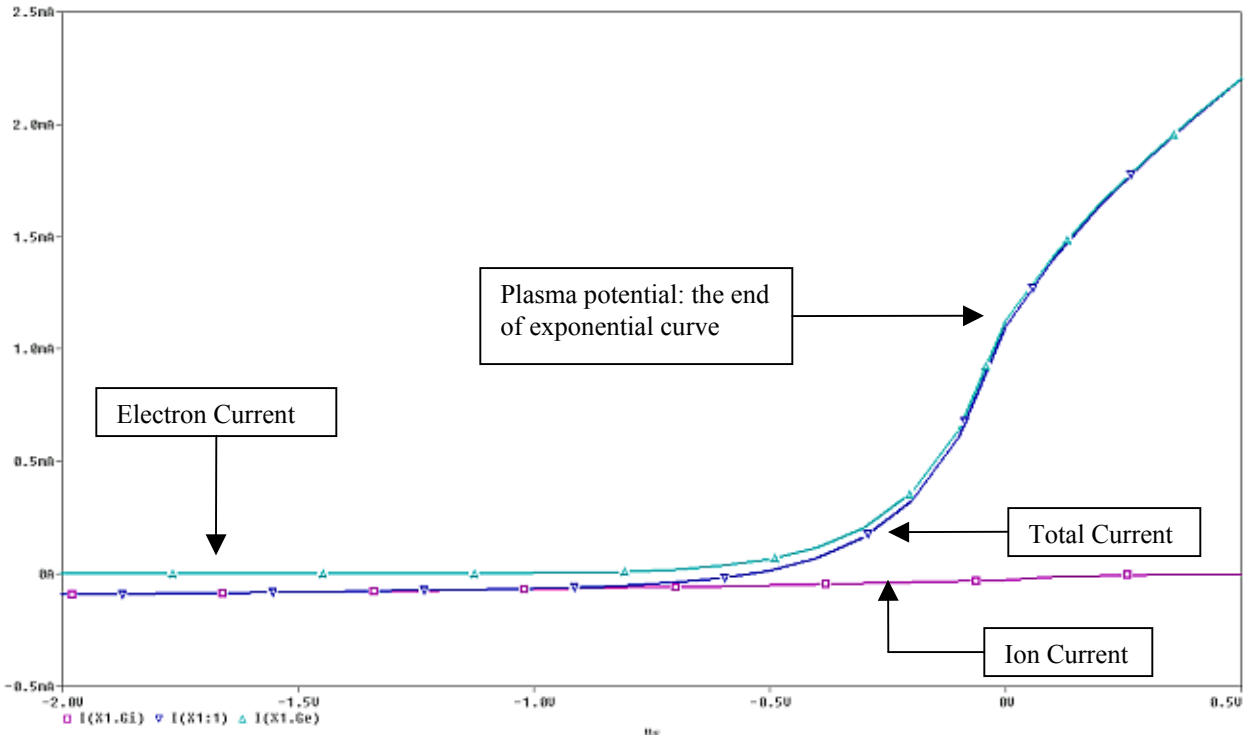

Figure 4. The I-V plot of the cylindrical probe

due to electrons and ions is zero. The model user does not need to bother about the complexity of nonlinear equations as the number of elements in the model increase. This capability becomes a boon when the model is expanded to include multiple number of dielectric surfaces, electric probes and biased solar array. Where mathematical simulation would lead to solving a complexly coupled nonlinear differential equations, the SPICE model is just a couple of lines long, iteratively calling the sub-circuit model for each of the elements.

A sub-circuit of the type shown in Figure 3 can be modeled for each of the geometries: plate, cylinder and sphere, by specifying the current sources with equations appropriate for a particular probe geometry. The sub-circuits then take A, n_o, and T_e as parameters. Having area as a parameter gives the same sub-circuit capability to model various parts of spacecrafts. Hence, each of these sub-circuits can be used to model different parts of a big spacecraft that comes closest to the geometry of the sub-circuit model. Complex spacecraft geometry can be modeled using this method leveraging on the 30+ years of development of SPICE by the electrical engineering community. Seen from a different perspective, the sub-circuit is a function that can be called any number of times, with different function parameters, to model different elements in same environment or same part in different environments. Furthermore, a parametric analysis can be performed on the model with varying parameters like area or ambient density, giving plots of potential with respect to the parameter. The model can also be used to generate I-V plots.

As a test of the above model we do a SPICE DC sweep of the sub-circuit from –2.0 volts to 0.5 volts, in a general LEO environment with T_e=T_i=2050 K, A = 1m^2, and plasma density as 1e11 m^{-3}. We can then generate I-V plot showing not only the individual currents for both the ion

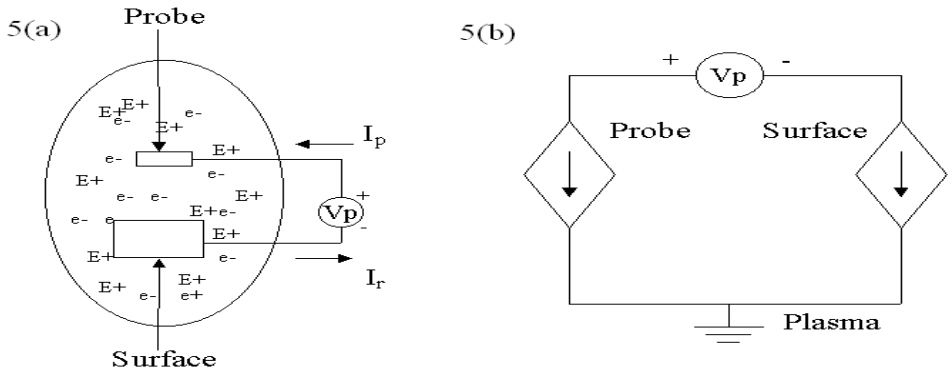

Figure 5. Spacecraft and attached Langmuir probe in plasma

and electron current sources but also the total current. The plot is shown in Figure 4. The curve is as expected from solving the equations manually or using any other mathematical models. The point where the total-current curve breaks away from an exponential rise is the plasma potential, and the point where the total current is zero (at -0.56V) is the floating potential. If we just need to find the floating potential without doing a voltage sweep or looking at plots, all that is required is to do a bias-point analysis and SPICE gives us the floating potential.

A very simple geometry of a spacecraft with a Langmuir probe be modeled as shown in Figure 5(a). The spacecraft and the probe are both assumed to be cylindrical but with significantly different surface areas. Each of these can be modeled using the cylindrical sub-circuit model with their areas passed as the parameter. The model can then be analyzed using SPICE as represented in Figure 5(b).

We can take the above simple example and expand it further to model the SAL rocket. The SAL rocket SPICE model is as shown in Figure 6. As above, plasma is modeled as the spacecraft ground. Node 'Surface' represents the spacecraft surface. Node 'DCP' is the DC Langmuir probe which is biased into the electron saturation region by 3 Volts relative to the spacecraft surface. Node 'FPP' represents the Floating Potential Probe, which were 4 identical carbon spheres extending out on the booms. Node 'FTP' is the Fast Temperature Probe. The FTP was designed [Siegfring et al., 1998] so as to keep it always biased in the electron retardation region. In order to avoid any effect of surface charging, FTP was biased by the amount that was the difference between the FPP and the spacecraft surface (V_{fpp}). It was then further biased by an additional volt. The dependence of the FTP bias on the voltage difference between the FPP and the spacecraft surface is modeled as Vd, which is a voltage-dependent-voltage-source with a 1:1 ratio to the voltage V(FPP - Surface). Cylindrical probe sub-circuit models the rocket surface and the DC probes, whereas spherical probe sub-circuit models the FPP and the FTP.

Each of the above sub-circuit models employ the standard colliosion-less plasma theory equations for the ions and the electrons which are modeled as thermal species. We realize that at this low altitude the plasma is cold and collisional, but our intention is to make a simple model to understand the behavior of the DC probe and not to quantitatively justify the collected current values. The plasma is considered collisional in cases where the mean free path is not greater then the spacecraft radius and the debye length. In the case when the mean free path is smaller then the spacecraft radius and is of the same order as the debye length, the current to a surface is just the collision-less scenario current scaled by a factor of lambda/a, where lambda is the mean free path and a is the spacecraft radius.

The ion thermal speed at T=180K is a maxwellian distribution around the mean value of 375 m/s. This is on the order of the rocket velocity, which is 660 m/s at 92 Km altitude. We thus chose to model the ions as a thermal species in our SPICE model of SAL. On the other hand, the dust being much heavier is relatively immobile and needs to be modeled as ram current. In the case of ram current, we assume the dust particle speed distribution to very narrow around the ram speed and therefore the current drops as a unit step function when the surface potential exceeds the directed ram energy. We then add another voltage-dependent-current-source in the sub-circuit models above for the dust ram current given by the following equation.

$$G_{dust}(V) = A_{ram}\, n_d\, Z_d\, V_{ram}\, H[\varepsilon - eV] \qquad V \geq Vp \tag{4}$$

$$G_{dust}(V) = A_{ram}\, n_d\, Z_d\, V_{ram} \qquad V \leq Vp \tag{5}$$

Where

A_{ram}	Cross-sectional surface area facing ram	V_{ram}	Spacecraft ram velocity
$n_d Z_d$	Dust charge density	V	Surface potential
e	Fundamental charge	V_p	Plasma potential (taken as 0V)

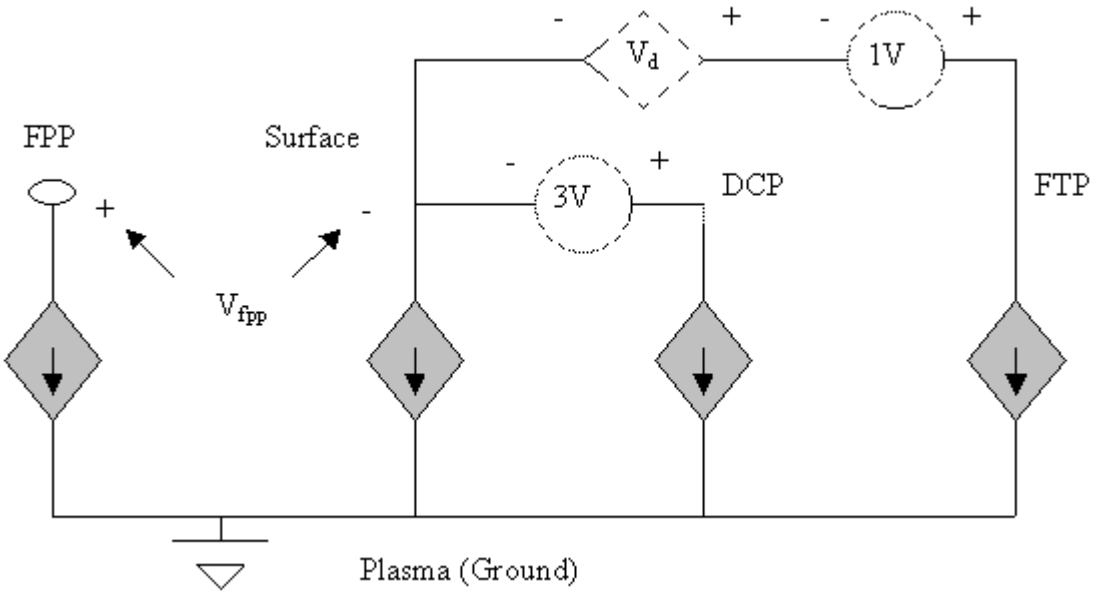

Figure 6. SAL rocket SPICE model

By the convention of our model, this current will be positive (going out) if the dust is negative and will be negative (coming in) if the dust is positive. We now pass additional parameters to the sub-circuits, the cross-sectional area A_{ram} and the dust charge density n_dZ_d. The energy ε is found using the relation (1/2) m v^2, where m is the mass of the dust and v is the rocket ram velocity.

Discussion

The charging of a dust particle due to collisions with ions and electrons leads it to acquire a negative charge, similar to a spacecraft acquiring a negative floating potential. On the other hand, charging by photoemission due to solar radiation leads to a positive charge on the dust. The SAL dust detector saw a layer of positively charged dust at an altitude of 92 Km, which coincides with the high electron density layer, observed by the SIP and the ground based lidar. The existence of positive dust at the same altitude with high electron density at nighttime is highly anomalous and is still not explicable. However we assume that the dominant charging process at the time of launch was photoemission, rather then electron attachment [Gelinas, 1999]. The fact that this high electron density layer disappeared shortly after the completion of the rocket flight (as observed by lidar) also indicates that it was indeed an artifact of photoemission from dust particles and later recombined as night progressed. If the high electron density was largely due to photoemission from dust particles, then it is safe to assume that at that altitude and at that time, the dust charge density constituted a higher percentage of positive charge density of the quasi-neutral plasma.

We define $\beta = (n_dZ_d / n_e) * 100$ as the percentage of positive charge attached to the dust. Where n_dZ_d is the dust charge density and n_e is the electron density. Figure 7 shows a plot of current observed in the DCP for the profile of electron density recorded by the SIP with varying β. As can be seen the higher the dust charge density the lower is the current observed. Comparing this with the Figure 2 where the DCP charged, it can be deduced that the dust layer present at 92 Km altitude had a high β rendering the fixed bias DCP and the vehicle surface unable to collect current from plasma.

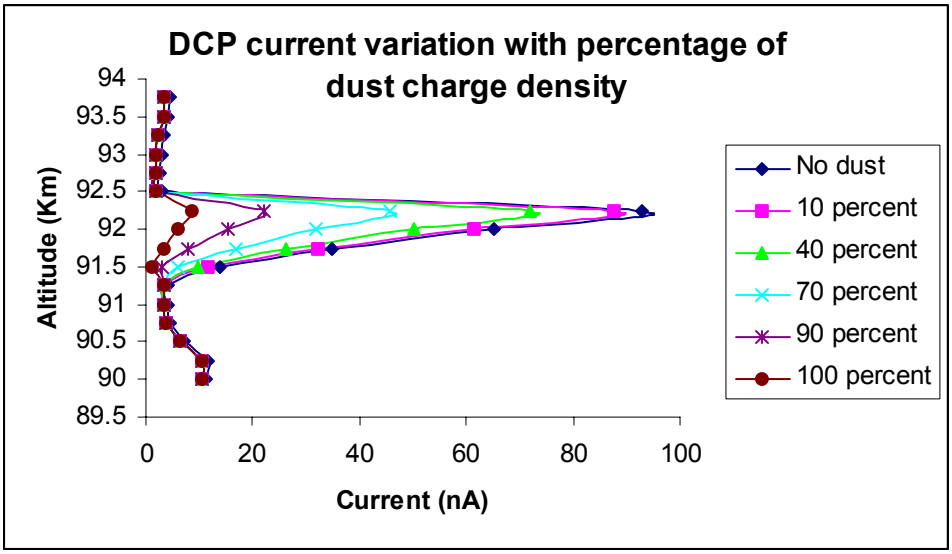

Figure 7. Variation in the current observed in the DCP with varying dust charge density as a percentage of total positive charge in the quasi-neutral plasma.

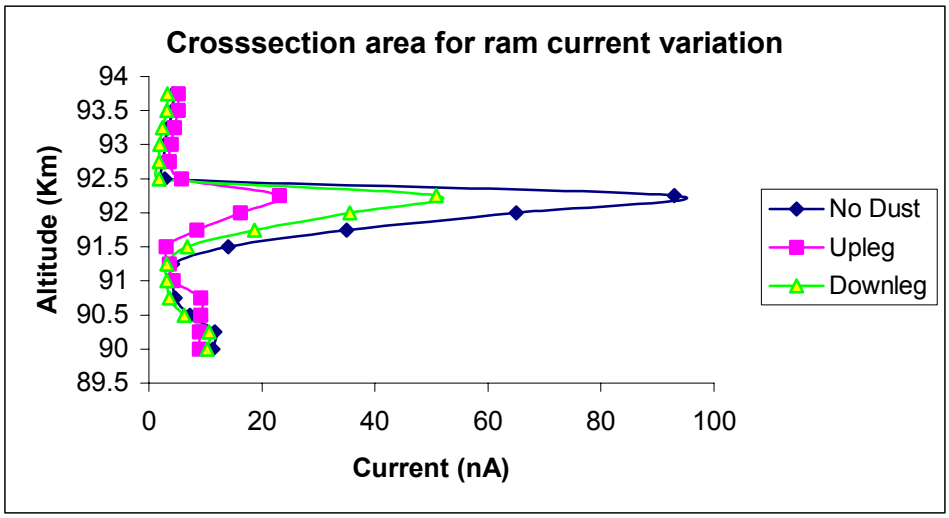

Figure 8. Variation in cross section area for the dust ram current leads to an over all variation in the total current.

Figure 7 explains why the DC probe registered a small electron density variation as compared to the SIP. It, however, does not explain why the upleg signal was fainter then the downleg signal. One of the simplest explanations could be the variation in the dust ram current collection due to rocket attitude variation between upleg trajectory and downleg trajectory. The rocket had an 8 degree inclination with the vertical during downleg, where as the inclination during upleg was only 2 degree. The variation in the ram area of the rocket was calculated based on this data and fed to the SPICE model. Two separate models were created, one each for upleg and downleg, with the only difference being the ram collection area for the dust current. The variation in the current collected by the DC probe is as shown in Figure 8. This plot, which was made assuming a β of 90% clearly shows us that the current collected during upleg will be lesser then the current collected on the downleg.

This feature is also explained in Figure 9. The Upleg shows us the upleg trajectory case when the inclination is 2 degrees to the vertical and hence the ram cross-section area is small. Due to a smaller ram cross-section area dust ram current is low and hence the rocket surface charges more negative to repel larger number of thermal electrons, leading to reduction in the current collected by the positive biased DC probe. The Downleg part shows us the downleg trajectory case when the inclination to the vertical was 8 degrees and the ram cross-section area increases by 3%. As the dust ram current collection is higher, the surface charges comparatively less negative and the current observed by the DC probe is higher. The interesting thing to note here is the fact that even 3% increase in cross-sectional area could lead to a significant change in floating potential.

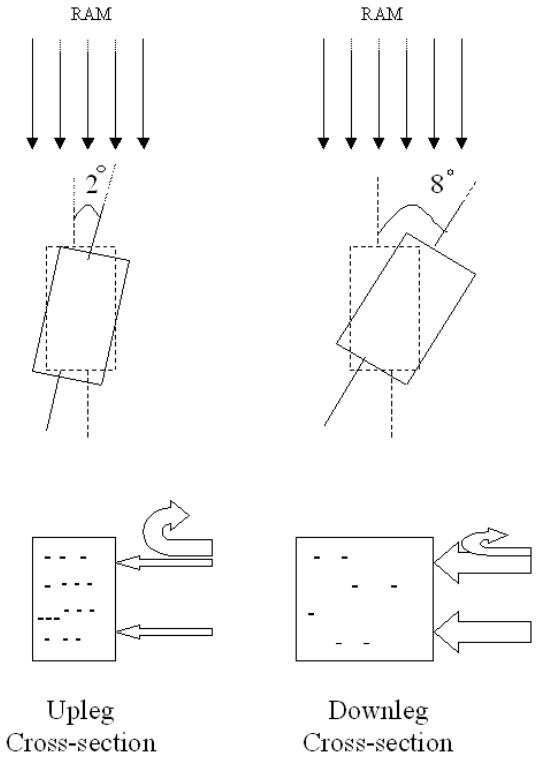

Figure 9. During Upleg the surface charges more negative to repel more electrons due to less positive charges striking its surface.

One of the things the model doesn't help us explain is the spike in the DCP observed current during the downleg trajectory. This phenomena is again shown in Figure 10, which is a zoomed in picture of the DCP collected current between the altitude of 90 to 100 Km. The same effect is observed in the upleg trajectory also although the effect is very subdued and the probe registers almost no current for the complete dust layer. One of the possible reasons for this difference between the upleg and downleg observations could be that the dust charge density is more at the bottom of the layer then at the top of the layer. This would lead to more surface charging during when the rocket hits the dust layer during its upleg trajectory. On the downleg trajectory the probe seems to track the high electron density layer for a very short time period, as shown by the spike, which slowly dies out even though the electron density layer continues further down. This feature of the observation is still not explicable. It seems that there is some capacitance in play during the charging event. We added the sheath capacitance parallel to the spacecraft surface in the SPICE model to try to model this transient effect. The sheath capacitance was calculated using the following equation:

$$C = \frac{\varepsilon \, \mathrm{A}}{\lambda_{\mathrm{d}}} \tag{6}$$

Where

ε Permittivity of free space

A Surface area of the spacecraft

λ_d Debye length

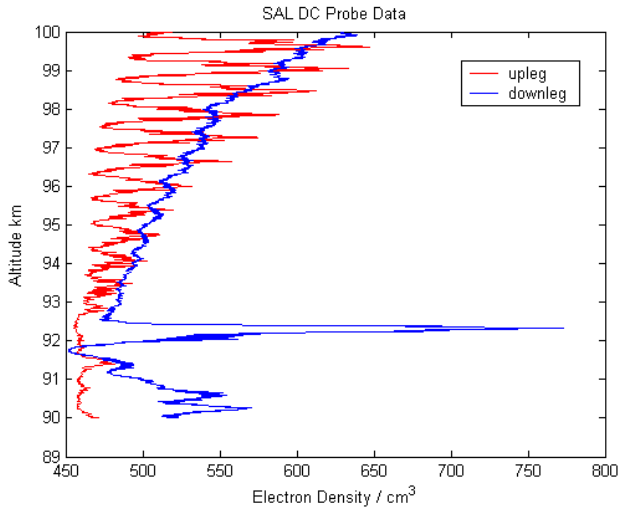

Figure 10. P current profile for upleg and downleg trajectory.

Using the sheath capacitance, the transient effect shown by the SPICE model is so short that complete profile generated using the model, sampling the current at the same rate as the actual probe, misses any transient effect. However, if the DCP current in the model is sampled faster we do see this transient effect. This transient effect, at the DCP sampling rate, is more visible in the model if the sheath capacitance is increased by a factor of 10. However, in order to observe the effect as shown in figure 10 the capacitance needs to be increased by a factor of 100, which seems unrealistic but could be possible. We are still looking into this feature of the observed DCP current profile.

Conclusion

In this work we have developed a simple SPICE model for spacecraft charging analysis that can be applied to various spacecraft geometries in varied conditions, in a relatively simple manner. This model can not only be used to evaluate and test electric probes on sounding rockets and satellites but also evaluate spacecraft charging for a particular spacecraft in specific orbital conditions. The model is largely for high-level understanding of the system characteristics and behavior with variations in plasma characteristics or spacecraft configuration. The model makes use of the existing theory for collision-less plasma, and as the theory for collision-less plasma is fairly robust the model itself also gives accurate representation of spacecraft charging. Although, if collisional plasma theory equations are developed carefully, then the model can also be used for fairly detailed analysis in collisional plasma conditions. This SPICE model can be used to emulate the behavior of fairly complex spacecraft by modeling various parts of the spacecraft as planar, cylindrical or spherical surfaces. The complex interdependence of the non-linear charging equations is solved by the numerical solver built with in SPICE, which has stood the test of time over the 30+ years of development in the industry.

This SPICE model was used to understand the anomalous behavior of the DC Langmuir probe on the SAL sounding rocket. The analysis done with the model tells us that for a sounding rocket to experience surface charging in a dusty plasma, the two important parameters are the percentage of positive charge density constituted by dust charge density, and the ram cross section of the rocket in the velocity direction. The higher the dust charge density percentage with

respect to the total positive charge, the higher the charging on the rocket surface. The higher the ram cross-section of the rocket surface, the lesser is the susceptibility of the surface to charging.

As SPICE is an electrical engineering tool, it is fairly simple to model transient effects of spacecraft charging by adding capacitors in the model. However, we are still trying to postulate a possible scenario to explain the spike in the DCP observed current during the downleg trajectory of the rocket.

References

1. Cen, F. F., Electric Probes, Chapter 4, Plasma Diagnostic Techniques, Edited by Huddlestone R.H. and Leonard S.L., Academic Press Inc. 1965.

2. DeForest, S.E., Spacecraft Charging at synchronous orbit, J. Geophys. Res., Vol. 77, No. 4, Feb, pp 651-659, 1972.

3. Frooninckx, T. B., and J. J. Sojka, Solar cycle dependence of spacecraft charging in Low Earth Orbit, J. Geophys. Res., Vol. 97, No. A3, Mar, pp 2985-2996, 1992.

4. Garrett, H.B. and A. C. Whittlesey, Spacecraft Charging, An update, IEEE Tran. Plasma Science, vol 28, no. 6, pp 2017-2028, Dec 2000.

5. Gelinas, L. J. et. al, First observation of meteoric charged dust in the tropical mesosphere, Gepphysical Research Letters, Vol 25, No. 21, 4047-4050, 1998.

6. Gelinas, L. J., An in-situ measurement of charged mesospheric dust during a sporadic atom layer event, University of New Hampshire, PhD Thesis, 1999.

7. Gussenhoven, M. S., D. A. Hardy, F. Rich, W. J. Burke and H. C. Yeh, High-level spacecraft charging in the low altitude polar auroral environment, J. Geophys. Res., Vol. 90, No. A11, Nov, pp 11,009-11,023, 1985.

8. Katz, I., and D. E. parks, Space Shuttle orbiter charging, J. Spacecr. Rockets, 20, 22, 1983.

9. Keown, J., OrCAD Pspice and Circuit Analysis, Fourth Edition, Prentice Hall, 2001

10. Pfaff, R.F., In-Situ measurement techniques for ionospheric research, Laboratory for extraterrestrial physics, NASA, 1996.

11. Rosen, A., Spacecraft charging: Environment-induced anomalies, J. Spacecr. Rockets, 13, 129, 1976.

12. Smithtro, C., and C. M. Swenson, A time dependent model of spacecraft charging with application to the International Space Station, AIAA Conf, 2002.